Luis A. Chavez*, Fabian O. Zayas Jimenez, Bethany R. Wilburn, Luis C. Delfin, Hoejin Kim, Norman Love and Yirong Lin

Characterization of Thermal Energy Harvesting Using Pyroelectric Ceramics at Elevated Temperatures

https://doi.org/10.1515/ehs-2018-0002

Abstract: Energy harvesting has drawn increasing attention due to the fast development of wireless sensors and devices. Most research has been focused on mechanical energy harvesting using piezoelectric ceramics; however, little is known on their experimental capabilities to harvest thermal energy at different temperature ranges and the impact that the temperature range has on the energy conversion efficiency. Majority of piezoelectric ceramics are pyroelectric in nature thus enabling them to couple energy between thermal and electrical domains. This paper demonstrates the use of Lithium Niobate (LNB) as a thermal energy harvesting device for high temperature applications. A custom testing setup was developed to test the LNB sample temperatures up to 225 °C. Pyroelectric coefficient of the material was characterized at different temperature ranges. Pyroelectric coefficient was found to increase with temperature, with a maximum value of $-196\,\mu C \cdot m^{-2}\,°C^{-1}$. Power output of the sample was also characterized in different temperature ranges. A maximum value of over 20.5 μW was found when cycling the sample between 75 °C and 100 °C. Meanwhile, a maximum value of 14.8 μW was found in the 125 °C to 150 °C range. Finally, a peak value of 255 nW was found when cycling the sample in the 200 °C to 225 °C range.

***Corresponding author: Luis A. Chavez,** Department of Mechanical Engineering, University of Texas at El Paso, El Paso, TX 79968, USA, E-mail: lachavez5@miners.utep.edu
Fabian O. Zayas Jimenez, Department of Mechanical Engineering, Universidad Del Turabo, Gurabo, PR 00778, USA, E-mail: fzayas7@email.suagm.edu
Bethany R. Wilburn: E-mail: brwilburn@miners.utep.edu, **Luis C. Delfin:** E-mail: lcdelfinmanriquez@miners.utep.edu, **Hoejin Kim:** E-mail: hkim4@miners.utep.edu, **Norman Love:** E-mail: ndlove@utep.edu, **Yirong Lin:** E-mail: ylin3@utep.edu, Department of Mechanical Engineering, University of Texas at El Paso, El Paso, TX 79968, USA

Keywords: thermal energy harvesting, energy harvesting at elevated temperatures, piezoelectric ceramics, pyroelectric characterization, harvester load optimization

Introduction

In recent years, there has been an increasing interest in developing functional materials and devices that can be used as sensors or energy harvesters in power plants (Kim et al. 2017a; Kim et al. 2017b; Cook-Chennault, Thambi, and Sastry 2008). Research in energy harvesting has been mainly focused on harvesting mechanical or thermal energy out of said systems (Cook-Chennault, Thambi, and Sastry 2008; Karim et al. 2016; Koumoto et al. 2013). Most of these efforts have been made at temperatures below 100 °C (Karim et al. 2016; Cuadras, Gasulla, and Ferrari 2010; Xie et al. 2010). However, most energy conversion environments operate at much higher temperatures (Rattner and Garimella 2011). Therefore, it is crucial to develop methods to harvest energy at higher temperatures that are closer to realistic systems. One of the limitations of energy harvesting at high temperatures is that almost all pyroelectric materials have Curie temperatures below 500 °C (Bowen et al. 2014). Furthermore, even fewer materials can retain pyroelectric properties when subject to temperatures over 650 °C, typical working temperatures of energy conversion systems such as exhaust from gas turbines (Rattner and Garimella 2011). Therefore, based on our previous success in demonstrating Lithium Niobate for high temperature sensors above 600 °C (Sarker et al. 2017), this manuscript presents the use of Lithium Niobate (LNB, Curie temperature 1100 °C) to harvest thermal energy at high temperatures using the pyroelectric effect.

Pyroelectricity is the change of spontaneous polarization of a range of dielectric materials due to changes of temperature across them. The change in polarization inside the material produces a flow of charges through its surfaces. This flow of charges is due to charge separation produced by the electrical displacement, which is at its turn produced by the change in temperature within

the material. This charge flow generated is described in eq. (1) (Yang et al. 2012),

$$i_p = \frac{dQ}{dt} = Ap\frac{dT}{dt} \quad (1)$$

where electrical current generated due to the pyroelectric effect is denoted as i_p, A is the surface area on an electrode, p is the pyroelectric coefficient, and dT/dt is the rate of change of temperature with respect to time.

Pyroelectric materials have been successfully used as temperature sensing devices (Tsai and Young 2003; Sarker et al. 2015; Ferrari et al. 2003). The electrical energy generated by pyroelectric materials has also been used as the energy source for small electronics, and has also been stored using commercial capacitors and supercapacitors (Yang et al. 2012). However, these projects used materials that contained lead and/or other materials that are not compatible with high temperatures. The constant need to utilize lead-free energy harvesting materials, as well as find materials that can provide reliable power output at extreme conditions is another benefit of the material presented in this paper. LNB has previously been used as a pyroelectric energy harvesting device at low temperatures (Karim et al. 2016).

In this paper, we report the use of LNB as a lead-free alternative for high temperature pyroelectric energy harvesting. A custom heating and cooling testing setup was utilized to characterize the power output of the material at different temperature ranges. The harvesting capability of the sample is demonstrated by measuring the power output utilizing different electrical resistive loads.

Methods

Sample

The sample used was a Z-cut LNB wafer from Precision Micro-Optics LLC. Top and bottom surfaces of the wafer were coated with silver paint (SPI Supplies, 05002-AB), which was then cured in an oven at 200 °C for 10 minutes on each side. The silver paint coatings served as electrodes for the sample. Physical properties of the sample used are listed in Table 1.

Table 1: Physical properties of LNB sample used in this study.

Sample properties	
Name	**Lithium Niobate**
Diameter (mm)	76.2
Thickness (mm)	0.5
Pyroelectric Coefficient (C/K·m^2)	-8.3×10^{-5}
Curie Temperature (°C)	1133 ± 3
Melting Point (°C)	1253
Density (g/cm^3)	4.647
Heat Capacity (J/K·mol)	89
Capacitance (F)	2.319×10^{-9}
Resistance (Ω)	9.349×10^{5}

Testing Setup

In order to create a controlled temperature environment on the sample, a custom testing setup was created. This testing setup is shown in Figure 1 and consisted of an axial fan attached to a metal duct, a 6×6 in. heating plate, and heat sink. An Arduino UNO R3 microcontroller was used to control the fan and heating elements to create a heating and cooling environment. The sample was heated by conducting heat from the embedded heaters to the heating plate, and was cooled through forced convection using ambient air aided by the axial fan and the heat sink.

Testing parameters such as temperature ranges and number of cycles were inputted into the microcontroller. The microcontroller then turned on the heating elements while keeping the cooling fan off until the upper

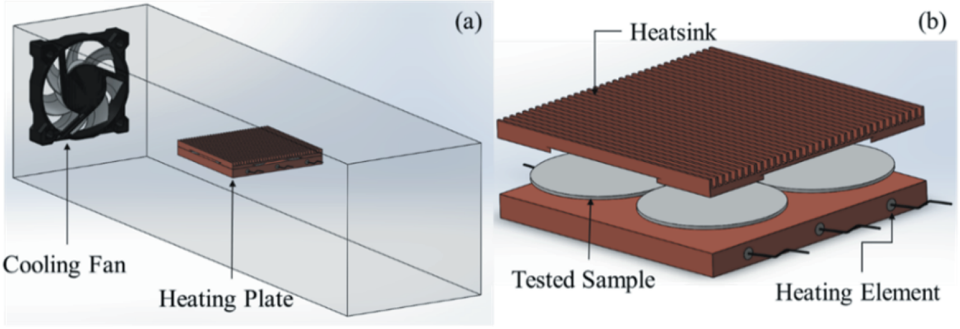

Figure 1: (a) Overview of testing setup and (b) close-up of heating plate and heatsink.

temperature limit was reached. Once this upper temperature limit was achieved, cooling fan was turned on while keeping the heating elements off until the lower temperature limit was reached. This process represented one full cycle and was repeated for the number of cycles previously specified. This testing setup was used to heat and cool the LNB sample to temperatures ranging from 75 °C to 225 °C. The sample was cycled in 25 °C intervals, starting in the 75 °C to the 100 °C range, until the upper limit of 225 °C was reached. The sample was cycled for a minimum of 5 heating and cooling cycles for each temperature range.

Current and Power Measurements

The sample was connected to different resistors to characterize the power output. A Keithley 6485 picoammeter was connected in series to the resistors and sample, and used to measure and record the current flowing through the circuit. Power was calculated using eq. (2) (Shu and Lien 2006),

$$P = I^2 \cdot R \tag{2}$$

where P is power, I is the current flowing through the circuit, and R is the applied resistance. This method to measure power output has been described in literature and commonly used to characterize power output in other energy harvesting research efforts (Sodano, Inman, and Park 2005; Granstrom et al. 2007; Leadenham and Erturk 2014).

A schematic of the measurement mechanism is found in Figure 2. LNB represents the sample, R_L is the applied electrical load, and A represents the picoammeter device used to measure the current. R_L was varied throughout the tests to determine the optimum load that led to the most power. In addition, the LNB wafer was directly connected to the picoammeter when characterizing the close circuit current output of the sample, and R_L was assumed to be equal to zero.

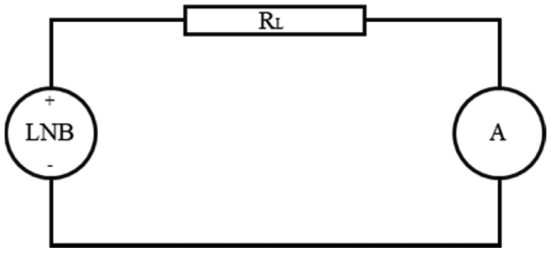

Figure 2: Schematic of current and power measurement circuit.

Results and Discussion

First, the pyroelectric current output from the sample at different temperature ranges was measured. The sample was cycled in 25 °C intervals, with temperatures ranging from 75 °C to 225 °C. Figure 3 shows the current output as heating and cooling cycles are introduced in the temperature range of 75 °C to 100 °C. The same process was performed at the other temperature ranges and a similar trend was followed. The current clearly followed the thermal stress introduced to the sample both in profile and intensity. A summary of the current output, as well as the dT/dt at these temperature ranges is shown in Figure 4. It is important to note that only the output values from the heating cycles were used. Additionally, the results shown are the average values throughout these heating cycles, and not peak values. The highest current output was found to be 157 nA, at the lowest temperature range.

It can be seen in Figure 4 that current decreases as temperature increases. However, it is observed that the temperature rate of change over time also decreases. This phenomenon is due to the testing setup being open to the environment and subject to natural convection. Therefore, results needed to be normalized to be able to properly characterize the response of the sample. The response was normalized by calculating the pyroelectric coefficient of the sample at different temperature ranges, and using this parameter as a comparison for different ranges. Pyroelectric coefficient is known to change as a function of temperature range and has been characterized for other materials in the past as well as for LNB in this temperature rage (Sarker et al. 2017; Newsome and Andrei 1997).

Using the results from Figure 4, the pyroelectric coefficient of the sample at these temperature ranges was calculated. This was done by using eq. (1) and solving for p. Pyroelectric coefficient as a function of temperature range is shown in Figure 5. It can be seen that the pyroelectric coefficient of the sample increases as temperature increases, which is in agreement to what is reported in literature (Whatmore 1986). A minimum pyroelectric coefficient of −100 $\mu C \cdot m^{-2} \cdot °C^{-1}$ was found at the lower temperature range. This value is similar to the one reported in literature of −83 $\mu C \cdot m^{-2} \cdot °C^{-1}$ (Bowen et al. 2014). The maximum value for the pyroelectric coefficient of −196 $\mu C \cdot m^{-2} \cdot °C^{-1}$ was found at the 200 °C to 225 °C range, which represents a 96 % increase of the pyroelectric coefficient compared with the room temperature value.

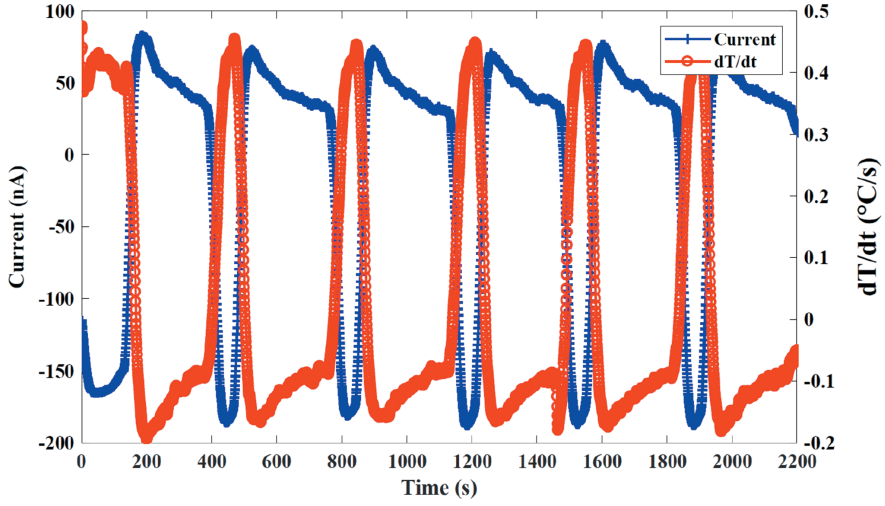

Figure 3: Current and dT/dt plotted against time for a temperature range of 75 to 100 °C.

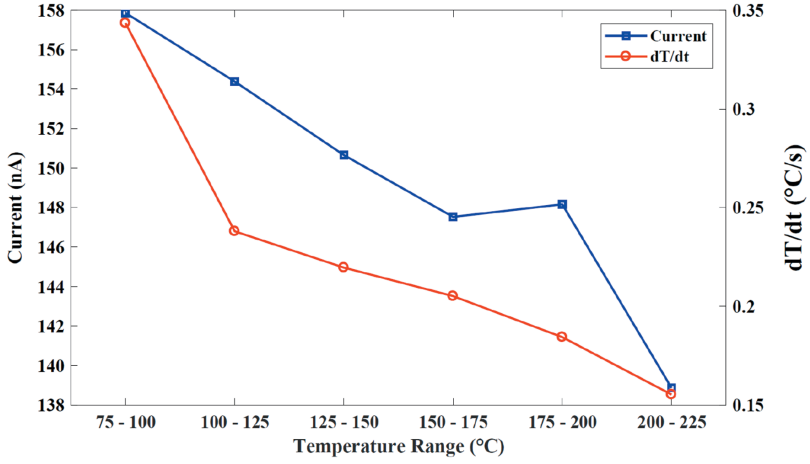

Figure 4: Average current and temperature change over time for different temperature ranges.

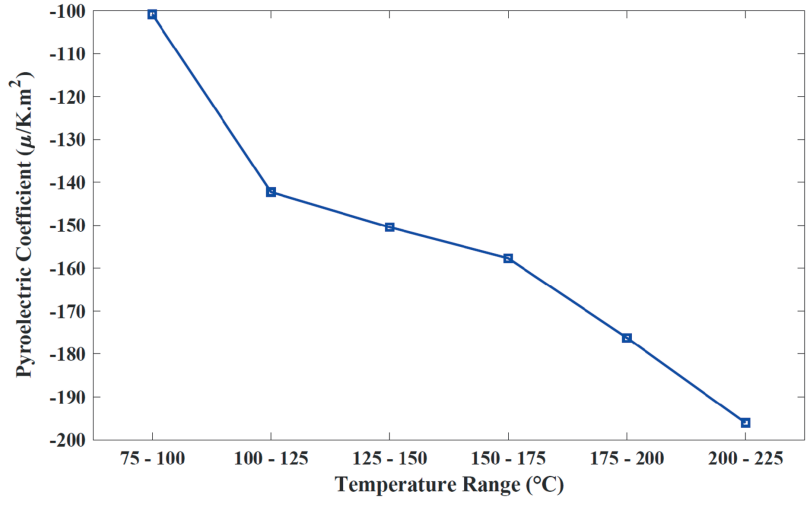

Figure 5: Pyroelectric coefficient as a function of temperature.

Once the response of the sample under no electrical load was characterized, the power generated under different electrical loads was measured. Three temperature ranges were selected for the characterization. The ranges selected were the lower and higher ranges, 75 °C to 100 °C and 200 °C to 225 °C, as well as an intermediate temperature range of 125 °C to 150 °C. The load was increased gradually using commercially available 10 MΩ

resistors to characterize the power output of the sample. Current generated by the sample at different temperature ranges as a function of load is shown in Figure 6. Figure 7 shows the power output of the sample for the different temperature ranges, as well as the experimental error found during these tests. Bias error was determined using manufacturer specified uncertainties and a Student's t-distribution assuming a 95% confidence interval was used to estimate random error.

As noted before, electrical resistive load was gradually increased. As seen in Figure 6, current decreases as temperature increases under the same load. It can also be seen that current drops faster as load is increased when testing at high temperatures. In order to harvest the higher power possible, output impedance of the sample and the impedance of the load must be matched (Liao and Sodano 2008). Impedance of the sample is dependent on material properties such as capacity and resistance, as a result LNB impedance peak values decrease as temperature increases (Kirk, et. al. 2015). Lower impedance values combined with lower current outputs resulted in lower overall power outputs. Therefore, although current increased at higher temperature under same temperature change rates, peak power will decrease as temperature increases. As a result, power continued increasing even under the highest resistance tested for the 75 °C to 100 °C and 125 °C to 150 °C ranges. As seen in Figure 7, maximum power occurred at 1 GΩ, for these two ranges. A maximum power of 20.5 μW was found for the 75 °C to 100 °C range and a maximum power of 14.8 μW at the125 °C to 150 °C range. The same method was used to characterize the power generated by the sample in the 200 °C to 225 °C range. Results for this test are shown in Figure 8.

Figure 8 presents the trend for the 200–225 °C temperature range since it is not clearly visible from the previous figure. The power generated in Figure 8 demonstrates an initial increase in power followed by a decreasing trend when tested under the high loads used for the other temperature ranges. The peak value is clearly seen and is below 100 MΩ. The peak values were not visible for

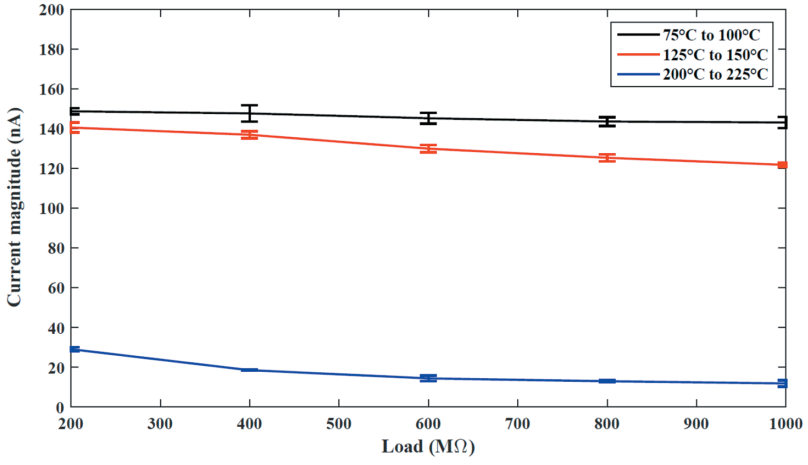

Figure 6: Current output for the different temperature ranges.

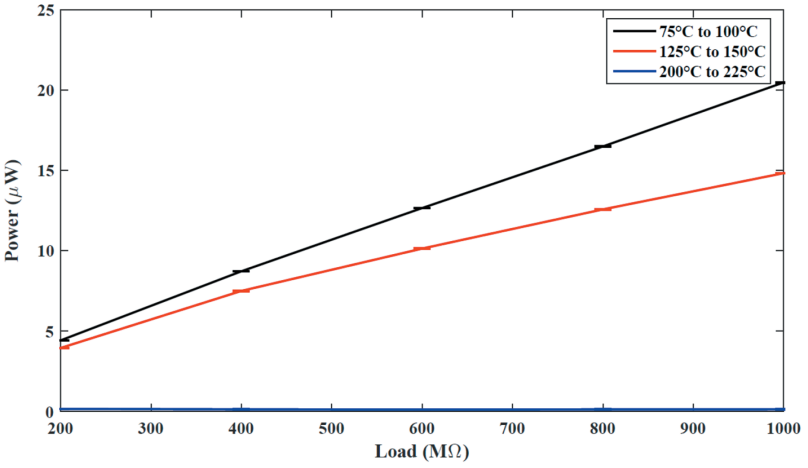

Figure 7: Power output at different temperature ranges.

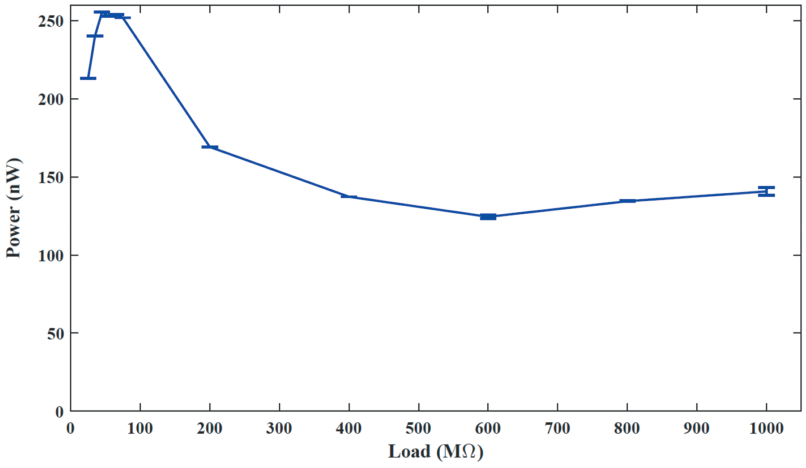

Figure 8: Average power output at 200 to 225 °C range.

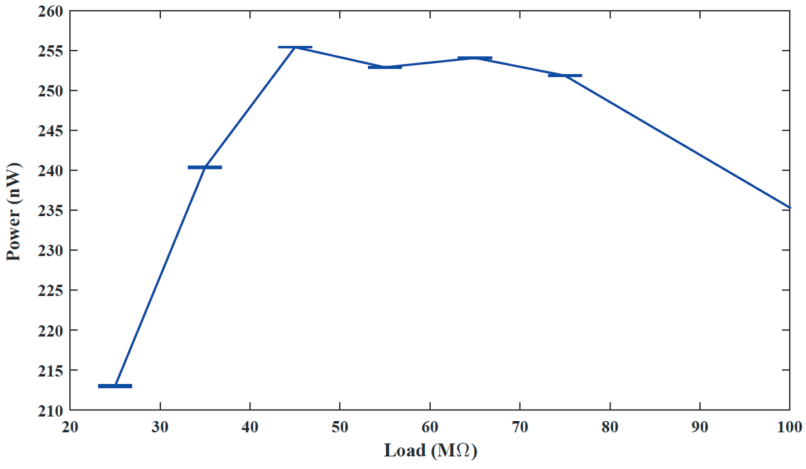

Figure 9: Peak power output at 200 °C to 225 °C temperature range.

the other temperature ranges; however, it is expected to have a similar trend at high resistive loads above 1 GΩ. A more detailed measurement of this temperature range is presented in Figure 9, which shows the power values when testing the sample under loads of 25 MΩ to 75 MΩ and a temperature range of 200 °C to 225 °C. An average peak power of 255 nW was found when applying a load of 45 MΩ. Lower power outputs are recorded at higher temperatures due to impedance matching effects. This trend is also seen in the plots of output current, Figure 4.

In addition to the impedance change of the sample due to temperature changes, the main contributing factor to the decrease of power output at higher temperatures was the decrease of pyroelectric power conversion efficiency. Pyroelectric power conversion efficiency is defined as the electrical work generated divided by the heat absorbed by the sample. Power conversion efficiency (ε) for pyroelectric materials is shown in eq. (3) (Fatuzzo, Kiess, and Nitsche 1966).

$$\varepsilon = \frac{AP_s(T^* - T_c)}{AP_s^2 T^* + C_p^{(0)}(T^* - T_c)} \tag{3}$$

where, A represents the initial state of the crystal, P_s represents the polarization, T^* is the temperature of the crystal, while T_c represents the Curie temperature of the material, and $C_p^{(0)}$ is the specific heat connected to the lattice alone. It can be seen that when the difference between the crystal and Curie temperature is large, the efficiency becomes equal to $AP_s^2/C_p^{(0)}$. Since both the state of the crystal and polarization stay constant throughout the whole cycle, the only factor contributing to the change in efficiency is the specific heat of the material. Specific heat of solids has been shown to increase as temperature increases (Raman 1956). This phenomenon effectively decreases the power conversion efficiency of the pyroelectric ceramic, further contributing to the overall lower efficiency observed during our measurements.

Using the previous results, peak power density of the sample was calculated at the different temperature ranges. The peak power at the tested temperature ranges was divided by the volume of the sample to obtain power density. Maximum power density at the 75 °C to 100 °C range was equal to 8.99 $\mu W/cm^3$. Meanwhile, a maximum power density of 6.49 $\mu W/cm^3$ at the 125 °C to 150 °C range was obtained. Finally, a peak power density of 111.84 nW/cm^3 was found at the 200 °C to 225 °C temperature range.

Summary and Conclusion

The feasibility of energy harvesting capabilities of a pyroelectric material capable of withstanding elevated temperatures was demonstrated. Pyroelectric coefficient characterization of the material in temperatures ranging from 75 °C to 225 °C was performed. The pyroelectric coefficient was found to increase as temperature rises with a maximum value of $-196\,\mu C \cdot m^{-2} \cdot °C^{-1}$ was found at the 200 °C to 225 °C range. Power outputs at low and high temperature ranges were obtained. A maximum value of over 20.5 μW was found when cycling the sample between 75 °C and 100 °C. Meanwhile, a maximum value of 14.8 μW was found in the 125 °C to 150 °C range. Finally, a peak value of 255 nW was found when cycling the sample in the 200 °C to 225 °C range. A decreasing power output at temperatures up to 225 °C was found due to a change in the impedance of the sample, as well as a lower pyroelectric power conversion efficiency at high temperatures due to an increase in the specific heat of the material. Despite a decrease in the pyroelectric power conversion efficiency was observed, the testing results demonstrated the feasibility of harvesting a still considerable amount of energy at different temperatures using $LiNbO_3$ piezoelectric ceramics.

Acknowledgements: This research is funded by Department of Energy (DOE) under Grant No. DE-FE0027502, and National Science Foundation (NSF) under NSF-PREM Grant No. DMR-1205302. Their financial support is greatly appreciated.

References

Bowen, C. R., J. Taylor, E. LeBoulbar, D. Zabek, A. Chauhan, and R. Vaish. 2014. "Pyroelectric Materials and Devices for Energy Harvesting Applications." *Energy & Environmental Science* 7 (12): 3836–3856.

Cook-Chennault, K. A., N. Thambi, and A. M. Sastry. 2008. "Powering MEMS Portable Devices—A Review of Non-Regenerative and Regenerative Power Supply Systems with Special Emphasis on Piezoelectric Energy Harvesting Systems." *Smart Materials and Structures* 17 (4): 043001.

Cuadras, A., M. Gasulla, and V. Ferrari. 2010. "Thermal Energy Harvesting through Pyroelectricity." *Sensors and Actuators A: Physical* 158 (1): 132–139.

Fatuzzo, E., H. Kiess, and R. Nitsche. 1966. "Theoretical Efficiency of Pyroelectric Power Converters." *Journal of Applied Physics* 37 (2): 510–516.

Ferrari, V., A. Ghisla, D. Marioli, and A. Taroni. 2003. "Array of PZT Pyroelectric Thick-Film Sensors for Contactless Measurement of XY Position." *IEEE Sensors Journal* 3 (2): 212–217.

Granstrom, J., J. Feenstra, H. A. Sodano, and K. Farinholt. 2007. "Energy Harvesting from a Backpack Instrumented with Piezoelectric Shoulder Straps." *Smart Materials and Structures* 16 (5): 1810.

Karim, H., M. R. H. Sarker, S. Shahriar, M. A. I. Shuvo, D. Delfin, D. Hodges, T. L. B. Tseng, D. Roberson, N. Love, and Y. Lin. 2016. "Feasibility Study of Thermal Energy Harvesting Using Lead Free Pyroelectrics." *Smart Materials and Structures* 25 (5): 055022.

Kim, H., F. Torres, D. Villagran, C. Stewart, Y. Lin, and T. L. B. Tseng. 2017a. "3D Printing of BaTiO3/PVDF Composites with Electric in Situ Poling for Pressure Sensor Applications." *Macromolecular Materials and Engineering* 302 (11): 1700229.

Kim, H., F. Torres, Y. Wu, D. Villagran, Y. Lin, and T. L. B. Tseng. 2017b. "Integrated 3D Printing and Corona Poling Process of PVDF Piezoelectric Films for Pressure Sensor Application." *Smart Materials and Structures* 26 (8): 085027.

Kirk, K. J., R. Hou, N. Schmarje, N. M. Pragada, L. Torbay, and D. Hutson. 2015. "Investigation of high-temperature ultrasonic transducer design using lithium niobate piezocomposite." *Insight – Non-Destructive Testing and Condition Monitoring* 57 (4): 193–199.

Koumoto, K., R. Funahashi, E. Guilmeau, Y. Miyazaki, A. Weidenkaff, Y. Wang, and C. Wan. 2013. "Thermoelectric Ceramics for Energy Harvesting." *Journal of the American Ceramic Society* 96 (1): 1–23.

Leadenham, S., and A. Erturk. 2014. "M-Shaped Asymmetric Nonlinear Oscillator for Broadband Vibration Energy Harvesting: Harmonic Balance Analysis and Experimental Validation." *Journal of Sound and Vibration* 333 (23): 6209–6223.

Liao, Y., and H. A. Sodano. 2008. "Model of a Single Mode Energy Harvester and Properties for Optimal Power Generation." *Smart Materials and Structures* 17 (6): 065026.

Newsome, R. W., and E. Y. Andrei. 1997. "Measurement of the Pyroelectric Coefficient of Poly (Vinylidene Fluoride) down to 3 K." *Physical Review B* 55 (11): 7264.

Raman, C. V. 1956. "The Specific Heats of Crystals." *Proceedings Mathematical Sciences* 44 (6): 367–374.

Rattner, A. S., and S. Garimella. 2011. "Energy Harvesting, Reuse and Upgrade to Reduce Primary Energy Usage in the USA." *Energy* 36 (10): 6172–6183.

Sarker, M. R. H., H. Karim, R. Martinez, D. Delfin, R. Enriquez, M. A. I. Shuvo, N. Love, and Y. Lin. 2015. "Temperature

Measurements Using a Lithium Niobate (Linbo3) Pyroelectric Ceramic." *Measurement* 75: 104–110.

Sarker, M. R. H., J. L. Silva, M. Castañeda, B. Wilburn, Y. Lin, and N. Love. 2017. "Characterization of the Pyroelectric Coefficient of a High-Temperature Sensor." *Journal of Intelligent Material Systems and Structures*, 1045389×17721376.

Shu, Y. C., and I. C. Lien. 2006. "Analysis of Power Output for Piezoelectric Energy Harvesting Systems." *Smart Materials and Structures* 15 (6): 1499.

Sodano, H. A., D. J. Inman, and G. Park. 2005. "Generation and Storage of Electricity from Power Harvesting Devices." *Journal of Intelligent Material Systems and Structures* 16 (1): 67–75.

Tsai, C. F., and M. S. Young. 2003. "Pyroelectric Infrared Sensor-Based Thermometer for Monitoring Indoor Objects." *Review of Scientific Instruments* 74 (12): 5267–5273.

Whatmore, R. W. 1986. "Pyroelectric Devices and Materials." *Reports on Progress in Physics* 49 (12): 1335.

Xie, J., X. P. Mane, C. W. Green, K. M. Mossi, and K. K. Leang. 2010. "Performance of Thin Piezoelectric Materials for Pyroelectric Energy Harvesting." *Journal of Intelligent Material Systems and Structures* 21 (3): 243–249.

Yang, Y., W. Guo, K. C. Pradel, G. Zhu, Y. Zhou, Y. Zhang, Y. Hu, L. Lin, and Z. L. Wang. 2012. "Pyroelectric Nanogenerators for Harvesting Thermoelectric Energy." *Nano Letters* 12 (6): 2833–2838.